European Journal of Neuroscience, Vol. 17, pp. 1581–1590, 2003

A hot spot for *hotfoot* mutations in the gene encoding the δ2 glutamate receptor

Ying Wang,[1] Shinji Matsuda,[1] Valerie Drews,[2] Takashi Torashima,[1] Miriam H. Meisler[2] and Michisuke Yuzaki[1]
[1]Department of Developmental Neurobiology, St. Jude Children's Research Hospital, Memphis, TN 38105, USA [2]Department of Human Genetics, The University of Michigan, Ann Arbor, MI 48109, USA

Keywords: assembly, ataxia, cerebellum, mutant, Purkinje cells

Abstract

The orphan glutamate receptor δ2 is selectively expressed in Purkinje cells and plays a crucial role in cerebellar functions. Recently, ataxia in the *hotfoot* mouse *ho4J* was demonstrated to be caused by a deletion in the δ2 receptor gene (*Grid2*) removing the N-terminal 170 amino acids of the δ2 receptor. To understand how δ2 receptors function, we characterized mutations in eight additional spontaneously occurring *hotfoot* alleles of *Grid2*. The mouse *Grid2* gene consists of 16 exons, spanning approximately 1.4 Mb. Genomic DNA analysis showed that seven *hotfoot* mutants had a deletion of one or more exons encoding the N-terminal domain of δ2 receptors. The exception is *ho5J*, which has a point mutation in exon 12. Deletions in *ho7J, ho9J*, *ho11J* and *ho12J* mice result in the in-frame deletion of between 40 and 95 amino acids. Expression of constructs containing these deletions in HEK293 cells resulted in protein retention in the endoplasmic reticulum or *cis*-Golgi without transport to the cell surface. Coimmunoprecipitation assays indicated that these deletions also reduce the intermolecular interaction between individual δ2 receptors. These results indicate that the deleted N-terminal regions are crucial for oligomerization of δ2 receptors and their subsequent transport to the cell surface of Purkinje cells. The relatively large size of the *Grid2* gene may be one of the reasons why many spontaneous mutations occur in this gene. In addition, the frequent occurrence of in-frame deletions within the N-terminal domain in *hotfoot* mutants suggests the importance of this domain in the function of δ2 receptors.

Introduction

The cerebellum plays a crucial role in controlling posture and smooth movement. Dysfunction of the cerebellum is typically manifested as ataxia, a common symptom of various neurological disorders in both mice and humans. There is now considerable evidence that the cerebellum is also involved in nonmotor functions and in a variety of neuropsychiatric disorders, such as dyslexia, autism and attention-deficit hyperactivity disorder (Berquin *et al*., 1998; Courchesne, 1999; Nicolson *et al*., 2001). An understanding of molecular mechanisms underlying ataxia may provide insight into normal and abnormal cerebellar functions, and permit the development of novel therapeutic approaches for specific disorders.

The ionotropic glutamate receptor family that mediates fast neurotransmission in vertebrate brain consists of the α-amino-3-hydroxy-5-methyl-4-isoxazolepropionate (AMPA) receptor, the kainate receptor and the *N*-methyl-D-aspartate (NMDA) receptor. On the basis of amino acid similarity, δ2 glutamate receptors have been classified as ionotropic glutamate receptors. Although δ2 receptors are predominantly expressed in postsynaptic densities of parallel fibre–Purkinje cell synapses in the cerebellum (Landsend *et al*., 1997), the mechanisms by which they participate in cerebellar function are largely unknown. When expressed alone or with other glutamate receptors, δ2 receptors do not form functional glutamate-gated ion channels or bind to glutamate analogues (Araki *et al*., 1993; Lomeli *et al*., 1993). Nevertheless, mutations in the δ2 receptor gene (*Grid2*) cause cerebellar ataxia in mice (Kashiwabuchi *et al*., 1995). For example, the ataxia of *lurcher* mice results from a point mutation in the *Grid2* gene; this dominant mutation causes constitutive activation of mutant δ2 receptors in the absence of ligand and eventually leads to the death of Purkinje cells (Zuo *et al*., 1997). Characterization of the *lurcher* mutation has indicated that δ2 receptors may act as ion channels, although the receptor ligand has not been identified (Kohda *et al*., 2000). At least 16 independent *hotfoot* mutants have been identified (Lalouette *et al*., 2001). Unlike the dominantly inherited *lurcher* allele, the *hotfoot* mutants carry recessive loss-of-function mutations that cause ataxia in the absence of obvious Purkinje cell death. The *ho4J* mutation produces a 170-residue deletion within an N-terminal extracellular leucine/isoleucine/valine-binding protein (LIVBP)-like domain of the δ2 receptor (Lalouette *et al*., 1998). We recently reported that the mutation in *ho4J* mice inhibits the function of δ2 receptors by impairing their exit from the endoplasmic reticulum (ER) (Matsuda & Yuzaki, 2002). We also identified the *in vitro* and *in vivo* functions of the LIVBP-like domain, which had not been well characterized in other glutamate receptors. Characterization of other naturally occurring *hotfoot* mutations may provide additional clues to the functions of the δ2 receptor and the roles of its various domains. The results of such characterization will provide a better understanding of the pathophysiology of ataxia.

In this paper, we report the alterations of the *Grid2* gene in seven previously identified *hotfoot* alleles: *ho5J*, *ho7J*, *ho8J*, *ho9J, ho11J*, *ho12J* and *ho13J*. We also characterize a newly identified allele designated *tapdancer* (*tpr*).

Correspondence: Dr M. Yuzaki, as above.
E-mail: michi.yuzaki@stjude.org

Received 27 November 2002, revised 18 February 2003, accepted 20 February 2003

doi:10.1046/j.1460-9568.2003.02595.x

Materials and methods

Mice and genomic DNA

Mice carrying the *ho5J* allele on the C57BL/6J background were purchased from the Jackson Laboratory (Bar Harbor, ME, USA). The *tap-dancer* allele (*tpr*) arose spontaneously on a mixed genetic background that included strain C57BL/10.JD2SnJ at the University of Michigan (Ann Arbor, MI, USA) and was provided by Drs Diane Robins and Arno Scheller. Genomic DNA from mice homozygous for the *ho7J* (TR/Di-Atp7a^{Moto}), *ho8J* (B10.D2/nSnJ), *ho9J* (B6.PL-Thy1^{a}), *ho11J* (C57BLKS/J-m+/+Lefr^{db}), *ho12J* (C57BLKS/J-m+/+Lefr^{db}) and *ho13J* (B10.D2/nSnJ) alleles were purchased from the Jackson Laboratory. All procedures related to the care and treatment of animals were according to NIH guidelines, and the experimental protocol was approved by the SJCRH Animal Resource Committee. Animals were killed by decapitation after anaesthetization with tribromoethanol.

Database searches and analysis of genomic sequences

The full-length gene for the δ2 receptor was identified by searching mouse genomic databases at the Mouse Genome Resources (National Center for Biotechnology Information) with the δ2 receptor cDNA as the query sequence. The exon–intron boundaries were determined by analysing the genomic DNA sequence with NetGene2 (The Technical University of Denmark, Lyngby, Denmark).

PCR analysis of genomic DNA

Genomic DNA was prepared from mouse tail by the HotSHOT method (Truett *et al.*, 2000). Polymerase chain reaction (PCR) was performed in a RoboCycler (Stratagene, La Jolla, CA, USA) with *Taq* DNA polymerase (Qiagen, Valencia, CA, USA) and primers designed from introns flanking each exon (Table 1). The schedule for PCR was as follows: preincubation at 94 °C for 5 min followed by 35 cycles in which each cycle consisted of incubation at 94 °C for 45 s, at 54 °C for 45 s and at 72 °C for 45 s. The last cycle was followed by a 5 min incubation at 72 °C. In reaction mixtures for the amplification of exons 5 and 6, 5% dimethylsulphoxide was included. The amplified DNA fragments were purified by using the MinElute PCR purification kit (Qiagen) and sequenced using the PCR primer.

Reverse transcriptase-PCR

We isolated total RNA from cerebella of wild-type and mutant mice using the RNeasy Protect Mini Kit (Qiagen). Trace amounts of genomic DNA were removed by digestion with DNAase (DNA-free; Ambion, Austin, TX, USA). The cDNA was prepared by reverse transcription (RT, RETROscript; Ambion) of total RNA with an oligo-dT primer. We used the oligonucleotides 5′-GCA TCG GAG GAT GGA AGT TTT CCC CTT GC-3′ and 5′-GCT GTC TGC TGC TCA TAT GG-3′ to amplify δ2 receptor cDNA. To confirm the *ho5J* mutation, another pair of primers 5′-GAT TGC AAA TGG GAT CGA TG-3′

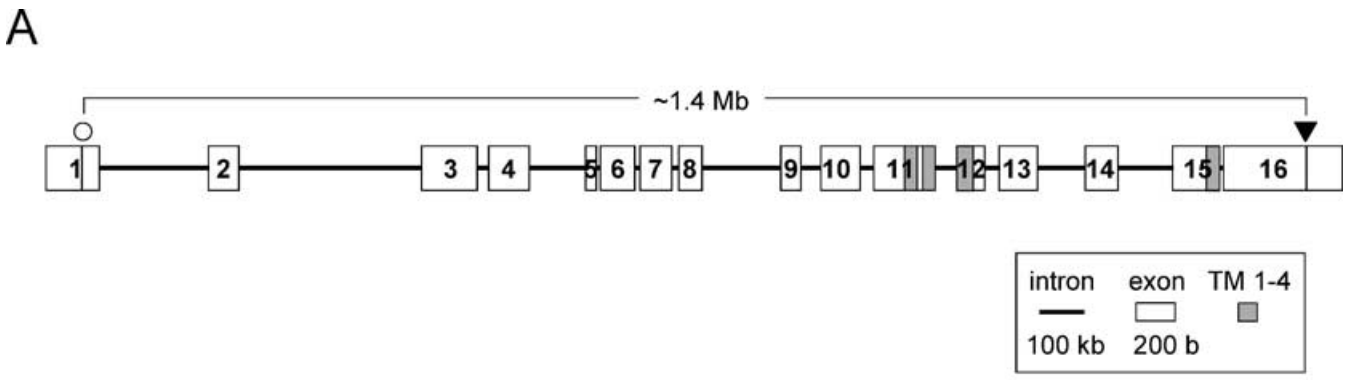

B

```
atcggcatcggaggatggaagt-(exon 1, >88 bp)-atccacatcg  GTaagacagg-(intron 1, ~246 kb)-
ttctttctAG  gagcaatttt-(exon 2, 156 bp)-gttcaagaag  GTaagtccat-(intron 2, ~408 kb)-
tctcttgcAG  catgtgaact-(exon 3, 285 bp)-agtgaatatg  GTaagtgttt-(intron 3, ~ 22 kb)-
ataatcctAG  atatccgtgg-(exon 4, 206 bp)-cataagtgag  GTaagcacta-(intron 4, ~125 kb)-
tctgttctAG  gtggtggaga-(exon 5,  54 bp)-cattaatgag  GTaaagccca-(intron 5, ~  8 kb)-
tatcttttAG  gaaataaatg-(exon 6, 174 bp)-gaatatggag  GTgggtctta-(intron 6, ~ 13 kb)-
ttctttccAG  atttctaacc-(exon 7, 162 bp)-catcaagaag  GTaactatct-(intron 7, ~ 17 kb)-
cctcatctAG  ggtggagtta-(exon 8, 120 bp)-tgtccgtaaa  GTaagcctga-(intron 8, ~188 kb)-
tgcctttcAG  cttgggtgct-(exon 9, 102 bp)-gactgtattg  GTaagcacca-(intron 9, ~ 44 kb)-
tgcctttcAG  cttgggtgct-(exon10, 198 bp)-gactgtattg  GTaagcacca-(intron10, ~ 25 kb)-
aatttcccAG  agagctgaca-(exon11, 313 bp)-gtacagcaag  GTaagagaaa-(intron11, ~ 49 kb)-
ctttccacAG  gtggggaagt-(exon12, 139 bp)-gctccatcca  GTaagtaggc-(intron12, ~ 35 kb)-
cctaatcaAG  gtctcttcag-(exon13, 196 bp)-cattcaaaag  GTactgtgct-(intron13, ~104 kb)-
aatttcacAG  gtaaaatatg-(exon14, 167 bp)-tttcacaaag  GTaaggctac-(intron14, ~130 kb)-
tcacccccAG  gatcctggag-(exon15, 241 bp)-atcgaaagag  GTacttgaac-(intron15, ~  2 kb)-
tcatctccAG  gatgacaagg-(exon16,>423 bp)-gtccatatgagcagcagacagc
```

FIG. 1. The *Grid2* gene: exon–intron organization. (A) The exon–intron organization of the mouse *Grid2* gene is shown schematically. Exons and introns are drawn according to different scales. The translational start and stop codons are indicated by ○ and ▼, respectively. Putative transmembrane regions (TM1–TM4) are indicated by shaded boxes. (B) The nucleotide sequences of all intron–exon junctions and all exon sizes and estimated intron sizes are listed. Splice donor (GT) and splice acceptor (AG) sites are underlined. The boldface type indicates the translational start codon (○) and the stop codon (▼).

TABLE 1. PCR primers used in this study

Region amplified by PCR	Sense	Antisense
Exon 1	GGGAAAGCTGCACTCAACTC	GCCACAGAAGCCCTGTCTTA
Exon 2	GCTTTCCCTGCAACAACAGT	ATGAGATGGCTCGGAGTGAT
Exon 3	CTCTTGCAGCATGTGAAC	CGCAGCTGACTAGACATC
Exon 4	CCTGCTTTTCCATCCCTCTT	CACTCTGCCTCCTTCATTAGTG
Exon 5	CGCTGCTTTGGTGATAGT	AGTGGCTGTTGATAGGAGAG
Exon 6	ATCGCTAAGGCCAACAAAGG	GATGCACCGTGGAAGATATACC
Exon 7	GCTGCCAAGCTGTCGTCACT	CACACCCACCTGCCTTCTCA
Exon 8	TGTGTCTCTTCCCTCATC	GCCCAACTGTCTGTCTAA
Exon 9	AAGGCCTCCACAGAGGTGAT	GAGGCTGGGCAACATGACTA
Exon 10	TGGGCTGATTAAGTACAGTTC	GTTTGGGGTAGGAGATATATG
Exon 11	AGTCCCTGCAGTACTTTC	GCCTGAGATCCACTAAGA
Exon 12	GTTGTCTGTCTTGGCACTGA	ATGTGCAGAGGGCTTTCCTT
Exon 13	GCAGTCCTCCTTAGCCATTA	GGGACCTGGAGTTTCCTTTA
Exon 14	CTCCACCACATGAAAGAG	ACCCACTTCTAGGAACTG
Exon 15	AAAGTCCCACCCACTCTGTT	GAGCAGTTGCCAATGTTACC
Exon 16	GGCCCAGTCAATATCTGCT	TCCATGTTAGTCCCACATTAC
Intron 2a	GGGAGTTGGGTTGGGCTGTA	GCAAGGACCGCAGTCAAGTG
Intron 2b	AGGCAGGTGGATGAAAGATG	TTGGGAGGGTCAGAACAAGA
Intron 4a	TCTGACCAGGACACTGGACAAT	GGGACAAAGGTGGGAAGAATGA
Intron 4b	CTTGGGCGAACTCATTACTG	GCACACCACGGTTAGATCAT
Intron 4c	AGGGATCTCCCAGTCCTTAC	GCCTCACCATTCACTGACTC
Intron 4d	AGTGCCACTTCATAGCGTCT	GGGCATTGGTAAAGGTACAG
Intron 6a	CTACTATACCCGGCCAAACT	CTGTTCTTGTGGCTGTCTTC
Intron 8a	CTACCCAGACCAGAAACAGT	CCCAGAGAAAGAGTTGAGAC
Intron 8b	GCTGCAGTGGCAGCAGACAAG	GAAAAGATCTGAAAGGAGTTGG
Intron 8c	CTCACAGGGTGTTGGTTGCTAA	TAAGCTGCCCATGTGACCATTG

and 5′-CAT CCC ATA CAA AAG CAT AG-3′ was used. To confirm the *tpr* mutation, a primer pair of exon 1-S (Table 1) and 5′-TCC TCC AGC TTC TTA TGG AA-3′ was used. PCR was performed by using *Taq* polymerase (Qiagen) for 35 cycles in which the annealing temperature was 60 °C. The absence of genomic DNA contamination was confirmed by performing PCR with an equivalent amount of total RNA but without RT.

Plasmid construction, transfection and immunoprecipitation

By using the modified overlap extension method and *Pfu* DNA polymerase (Stratagene, La Jolla, CA, USA), we introduced into the wild-type *Grid2* cDNA the deletions that we identified in the *ho7J* ($\delta2^{ho7J}$), *ho9J* ($\delta2^{ho9J}$) and *ho11J* ($\delta2^{ho11J}$) alleles. We placed cDNA that encoded a haemagglutinin (HA) or a FLAG tag immediately upstream of the stop codon of the wild-type δ2 ($\delta2^{wt}$), $\delta2^{ho7J}$, $\delta2^{ho9J}$ or $\delta2^{ho11J}$ cDNAs. These modified cDNAs, whose sequences were confirmed by bidirectional sequencing, were cloned into the expression vector pTracer-EGFP (Invitrogen, Carlsbad, CA, USA), and 10 μg of the plasmids was transfected into human embryonic kidney 293 (HEK293) cells by using the FuGENE transfection reagent (Roche, Indianapolis, IN, USA) or CellPhect transfection kit (Amersham Pharmacia, Piscataway, NJ, USA). The incubation of cells, the processing of samples and the immunoblotting analysis were performed as previously described (Matsuda & Yuzaki, 2002). Antibodies against the N-terminal region (a gift from Dr H. Hirai, RIKEN, Japan) or the C-terminal region (Chemicon, Temecula, CA, USA) of the δ2 receptor were used for immunoprecipitation or immunoblotting studies. For coimmunoprecipitation assay, antiHA (Covance, Richmond, CA, USA) and antiFLAG (Sigma, St. Louis, MO, USA) antibodies were used. Immunoblots were visualized with the ECL plus kit (Amersham Pharmacia) and exposed to an X-ray film within the linear range of reaction. Quantitative analysis was performed using the public domain NIH Image program (developed at the US National Institutes of Health and available on the Internet at http://rsb.info.nih.gov/nih-image/). The mean band intensity of FLAG-tagged $\delta2^{wt}$ receptors that coimmunoprecipitated with HA-tagged $\delta2^{wt}$ receptors was arbitrarily established as 100%.

Immunohistochemical analysis

To investigate the expression of δ2 glutamate receptors on the cell surface, we added cDNA encoding an HA tag to the 5′ end of the $\delta2^{wt}$ and mutant δ2 receptor cDNAs immediately downstream of the signal sequence. The modified cDNAs were subcloned into the pTracer-nucGFP expression vector (Invitrogen), which expresses green fluorescent protein (GFP) that is targeted to the nucleus, and the resulting constructs were transfected into HEK293 cells (total amount of vector, 10 μg) in a 12-well culture dish (Corning). Cells were fixed, and in the absence of Triton X-100, nonspecific binding sites were blocked with a solution containing 2% bovine serum albumin and 2% normal goat serum in phosphate-buffered saline (PBS). The cells were then incubated with antiHA antibody (Covance); bound antibody was detected by Alexa 546-conjugated secondary antibody (Molecular Probe, Eugene, OR, USA). Stained cells were visualized with a microscope (BX60; Olympus, Tokyo, Japan) equipped with a CCD camera (C5810; Hamamatsu Photonics, Shizuoka, Japan). Contrast or brightness adjustments were kept constant for quantitative analysis. The image analysis was performed using the NIH Image program. The average background red fluorescence was determined using HEK293 cells transfected with $\delta2^{wt}$ cDNA but incubated without the primary antibody. Cells displaying red fluorescence in the cytosol above the background level were counted as HA^{+}.

Glycosidase digestion

Endoglycosidase H (Endo H) digestion was performed as previously described (Matsuda & Yuzaki, 2002).

Structural modelling

The structural modelling of the LIVBP-like domain and statistical analysis were performed as previously described (Matsuda & Yuzaki, 2002).

Results

Genomic structure of the mouse δ2 glutamate receptor gene

The exon–intron structure of the mouse *Grid2* gene was determined by comparing *Grid2* cDNA with its genomic sequence obtained from mouse genomic databases (Fig. 1A). All exon–intron junctions were identical to canonical splice donor and acceptor sites (Fig. 1B). The receptor was encoded by 16 exons: the shortest (exon 5) encoded 17 amino acids and the longest (exon 16) encoded 141 amino acids (Fig. 1B). Several introns were quite large. The estimated lengths of intron 1 and intron 2 are 246 kb and 408 kb, respectively. Three other introns also exceed 100 kb in length. As a result, the entire gene covered a region of 1.4 Mb. In contrast, the average size of genes encoding glutamate receptors from other families is 190 ± 84 kb (mean $\pm$ SEM, $n = 18$). The largest gene, the kainate receptor GluR6, spans 690 kb; and the shortest, the NMDA receptor NR3B, spans 6 kb. The relatively large target size provided by the *Grid2* gene may be one of the reasons for the large number of spontaneous mutations.

Transmembrane domain 1 (TM1) and TM2 of δ2 receptors are encoded by exon 11, and TM3 is encoded by exon 12 (Fig. 1A). Although the number of exons and exon–intron positions vary among subunits of the glutamate receptor family, the exon–intron structure around exons encoding transmembrane domains is highly conserved in each family of glutamate receptors. For example, in the AMPA receptor family TM1 and TM2 are encoded by a single exon, whereas in the kainate receptor family each TM is encoded by a separate exon, and in the NMDA receptor NR2 subfamily TM2 and TM3 are encoded by a single exon. Although the δ2 receptor family is equidistant from the AMPA, kainate and NMDA receptor families in phylogenetic comparisons (Araki *et al*., 1993; Lomeli *et al*., 1993), the arrangement of exons encoding TMs suggests that the δ2 receptor family is most closely related to the AMPA receptor family.

Characterization of the ho5J allele: a point mutation in Grid2

The *ho5J* mutation arose at the Jackson Laboratory and has been used to establish the allelism of other *hotfoot* mutations (Dickie, 1966). To identify the mutation in *ho5J* mice, we performed RT-PCR of cerebellar RNA. The size of *ho5J* δ2 receptor cDNA was similar to that obtained from wild-type mice (Fig. 2A). Sequencing the amplified RT-PCR product revealed a single nucleotide deletion at position 1999, which is at the beginning of the region encoding TM3 (Fig. 2B). Sequencing of exon 12 amplified from genomic DNA confirmed the deletion of the guanine residue. The same result was obtained by using another pair of PCR primers, ruling out the possibility that the deletion was caused by PCR artefacts. This deletion is expected to cause a frame-shift and thus create a stop codon in the middle of the region encoding TM3 (Fig. 2C). Immunoblot analysis using antibodies against the N-terminal and C-terminal portions of δ2 receptors did

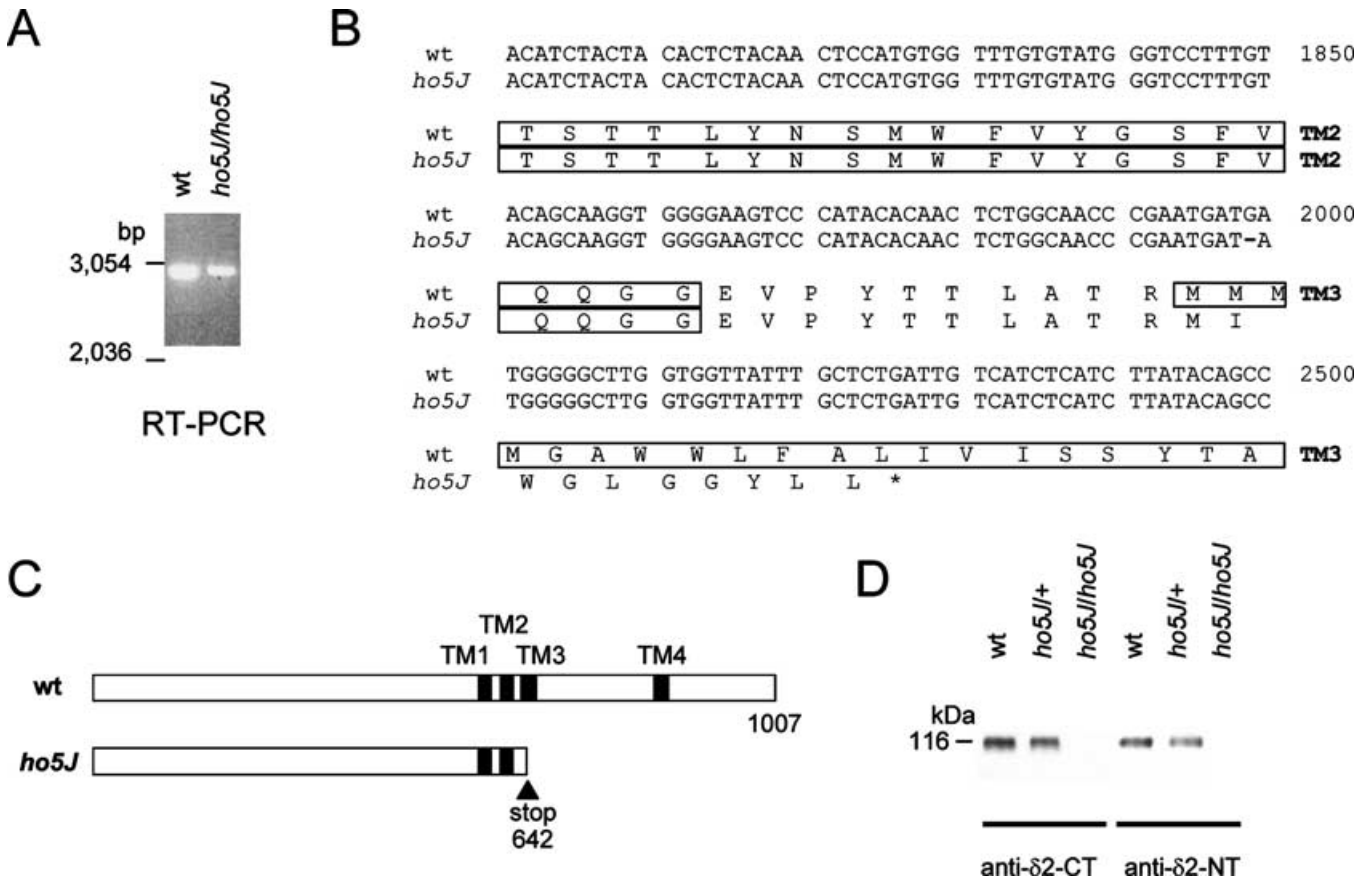

FIG. 2. Analysis of the *ho5J* allele. (A) Amplification of cerebellar mRNA from wild-type (wt) and *ho5J* homozygous mice by RT-PCR. In both cases, a 3.0-kb transcript was amplified. (B) A portion of the $\delta 2^{wt}$ and $\delta 2^{ho5J}$ cDNA and expected protein sequences. A single deletion at nucleotide position 1999 (nucleotide position 1 corresponds to the translational start codon) caused a frame-shift and thus created a stop codon in the middle of the region encoding TM3 in the *ho5J* allele. The numbers indicate the amino acid position (position 1 corresponds to the translational start point). (C) Schematic representation of the expected proteins encoded by wt and *ho5J* alleles. The positions of four transmembrane domains (TM1–TM4) are indicated. (D) Immunoblot analysis in which antibodies to the C-terminal region and the N-terminal region of the $\delta 2^{wt}$ receptor (antiδ2-CT and antiδ2-NT, respectively) were used. A 116-kDa protein was detected in wt and *ho5J* heterozygous cerebellar extracts, whereas no δ2 receptor protein was detected in cerebellar lysates of *ho5J* homozygotes.

not detect δ2 receptor protein in the cerebella of *ho5J* mice (Fig. 2D). Similarly, δ2 receptor protein was not detected when exon 12 of the *Grid2* gene was replaced with a neomycin transferase gene by homologous recombination (Kashiwabuchi *et al*., 1995). The lack of detectable protein suggests that the absence of TM3 and regions C-terminal to it make the δ2 receptor unstable and easily degraded.

Tapdancer is a new allele of Grid2

The *tpr* mutation was identified as a spontaneous mutation in the mouse colony at the University of Michigan. Affected mice exhibit the high-stepping gait (hypermetria) that is typical of *hotfoot* mutants (Fig. 3A). Despite their ataxic movement disorder, the life span of affected animals is normal. The frequency of affected F2 animals was 24% in a cross with strain C57BL/6J (22/93) and 20% in a cross with strain CAST/Ei (83/418), demonstrating autosomal recessive inheritance. The mutation was mapped by a genome scan experiment in which pooled DNA from 23 affected and 72 unaffected F2 mice was typed for 51 microsatellite markers spanning the mouse genome. Linkage was detected with markers from proximal chromosome 6. Genotyping of 26 affected F2 animals localized the mutation to a position approximately 30 cM from the centromere, with the following marker order and recombination frequencies: D6Mit154 – 5/52 – *tpr* – 1/52 – D6Mit16.

To test *Grid2* as a positional candidate gene, RT-PCR was performed on brain RNA. The length of the RT-PCR product from *tpr* brain was 491 bp shorter than the wild-type product (Fig. 3B). Sequencing of the RT-PCR product revealed the loss of sequences corresponding to exon 3 and exon 4, resulting in a frame-shift mutation and premature termination of translation at residue 91 in exon 5 (Fig. 3C). The same result was obtained by using another pair of PCR primers, ruling out the possibility that the deletion was caused by PCR artefacts. PCR amplification of genomic DNA demonstrated that exon 3 and exon 4 are deleted (Fig. 3D). The predicted truncated δ2 receptor (Fig. 3E) could not be detected by immunoblot analysis with antibodies against

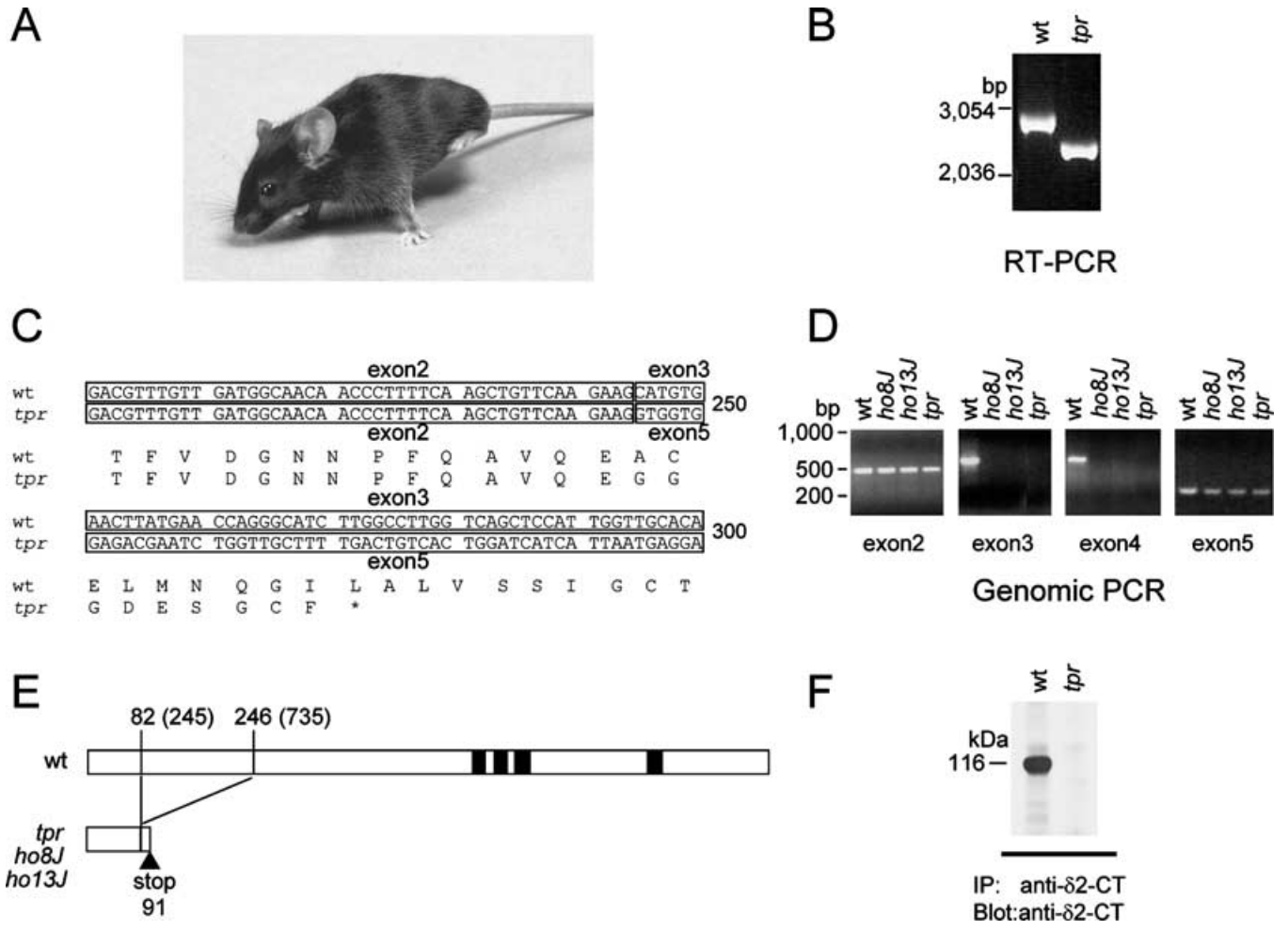

FIG. 3. Analysis of the *tpr*, *ho8J* and *ho13J* alleles. (A) Hypermetria of the hind limbs in *tapdancer* homozygotes. Hypermetria (high-stepping gait) is evident in this 3-month-old animal. The phenotype also includes ataxia, tremor, impaired balance, tendency to walk backwards, tapping of the hind limbs, hopping and splayed hind limbs. By 6 months of age, affected mice exhibit reduced mobility and flattened body posture. (B) PCR analysis of the *Grid2* gene. Genomic DNA from wild-type (wt) and homozygous *hotfoot* mice (*ho8J*, *ho13J* and *tpr*) was amplified by PCR in which primer pairs flanking exons 2, 3, 4 or 5 were used. Exons 3 and 4 were missing from these *hotfoot* alleles. (C) Schematic representation of the expected proteins encoded by wt and *ho8J, ho13J* and *tpr* alleles. The solid rectangles indicate the four transmembrane domains. Deletion of exons 3 and 4 is expected to cause a frame-shift and thus create a stop codon. The numbers in parentheses above the illustration of the wt protein indicate the corresponding nucleotide positions that serve as the beginning and endpoints of the region deleted from $\delta2^{tpr}$, $\delta2^{ho8J}$ and $\delta2^{ho13J}$ receptors. (D) Amplification of cerebellar mRNA from wt and *tpr* homozygous mice by RT-PCR. A deletion product of approximately 2.6 kb was detected in *tpr* cerebellar cDNA. (E) The cDNA and expected protein sequences of δ2 receptors in wt and *tpr* homozygous mice. A deletion between nucleotide positions 245 and 735 in the *tpr* allele is expected to cause a frame-shift and thus create a stop codon after nucleotide position 270. (F) Immunoblot analysis. Cerebellar extracts from wt and *tpr* homozygotes first underwent immunoprecipitation (IP) in which antibody to the C-terminal region of the $\delta2^{wt}$ receptor (anti-δ2-CT) was used; the immunoprecipitates were subjected to immunoblot analysis. No δ2 receptor protein was detected in *tpr* homozygotes.

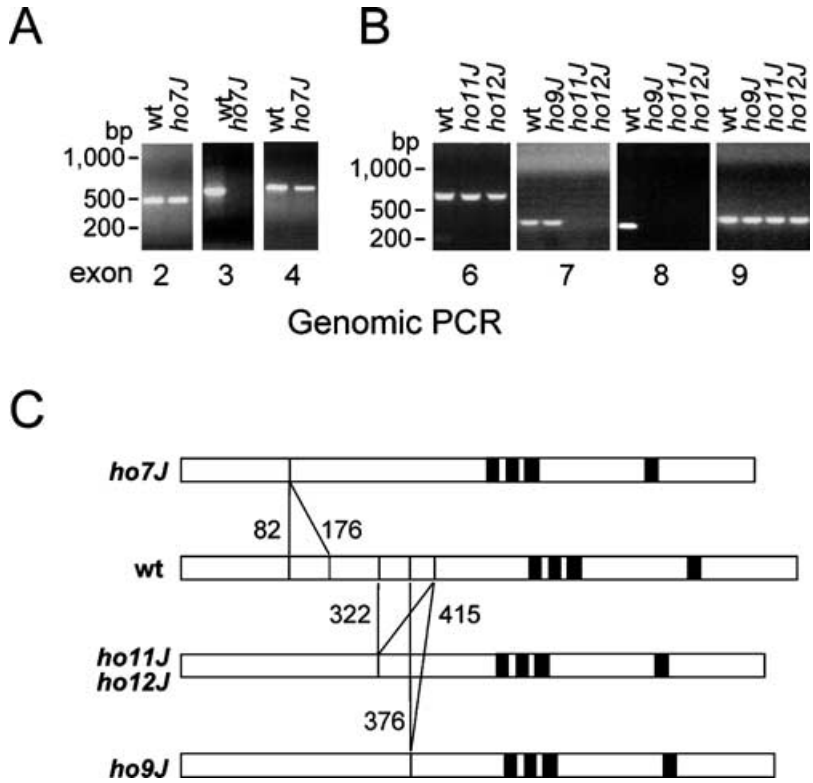

FIG. 4. Analysis of the *ho7J, ho11J, ho12J* and *ho9J* alleles. (A) PCR analysis of the *ho7J* allele. Genomic DNA from wild-type (wt) and homozygous *ho7J* mice was amplified by PCR using primer pairs flanking exons 2, 3 or 4. Exon 3 is missing from the *ho7J* allele. (B) PCR analysis of the *ho11J, ho12J* and *ho9J* alleles. Genomic DNA from wt and homozygous *hotfoot* mice (*ho11J*, *ho12J* and *ho9J*) was amplified by PCR using primer pairs flanking exons 6, 7, 8 or 9. Exons 7 and 8 were missing from the *ho11J* and *ho12J* alleles, whereas exon 8 was absent from the *ho9J* allele. (C) Schematic representation of the expected proteins encoded by the wt and the *ho7J, ho11J, ho12J* and *ho9J* alleles. Also shown are the start and endpoints (numbers indicate the amino acid position of wt protein, when position 1 corresponds to the translational start point) of each deleted region.

N-terminal and C-terminal portions of $\delta2^{wt}$ receptors (data not shown) or by immunoprecipitation with antiδ2 receptor antibody (Fig. 3F).

Exon deletion and frame-shift mutations in ho8J and ho13J

Although live mice colonies were unavailable, we were able to obtain genomic DNA for *ho7J*, *ho8J*, *ho9J*, *ho11J*, *ho12J* and *ho13J* mice. We analysed all exons of the *Grid2* gene from these mutant mice by PCR and subsequent sequencing. Using this approach, we confirmed the loss of exons 5–8 in *ho4J* genomic DNA (data not shown), as indicated by earlier RT-PCR analysis (Lalouette *et al*., 1998). Similarly, we detected a deletion of exons 3 and 4 in *ho8J* and *ho13J* genomic DNA (Fig. 3D). As described above for *tpr*, the absence of exons 3 and 4 results in a frame-shift and creates a stop codon at amino acid position 91 (Fig. 3E). No coding changes were observed in the non-deleted exons.

In-frame deletions in the LIVBP-like domain of δ2 receptors encoded by other hotfoot *alleles*

Genomic PCR demonstrated that exon 3 was missing in the *ho7J* allele of the *Grid2* gene (Fig. 4A). Similarly, exons 7 and 8 were absent in *ho11J* and *ho12J* alleles, and exon 8 was missing in the *ho9J* allele (Fig. 4B). The loss of these exons predicts in-frame deletions within the N-terminal LIVBP-like domain of the δ2 receptor protein: a 95-amino acid deletion in *ho7J* mice; a 94-amino acid deletion in *ho11J* and *ho12J* mice; and a 40-amino acid deletion in *ho9J* mice (Fig. 4C and D).

We previously demonstrated that the deletion in *ho4J* mice removed a 170-amino acid region in the LIVBP-like domain that is involved in the homomeric oligomerization of δ2 receptor proteins and subsequent transport of assembled proteins to the cell surface (Matsuda & Yuzaki, 2002). Therefore, we hypothesized that deletions within the LIVBP-like domain of δ2 receptors found in *ho7J*, *ho11J*, *ho12J* and *ho9J* mice also have similar effects. To test this hypothesis, we attached an HA tag to the N-terminus of each δ2 receptor with a unique mutation ($\delta2^{ho7J}$, $\delta2^{ho11J}$ and $\delta2^{ho9J}$) and expressed them in HEK293 cells. Under the nonpermeabilizing condition, the antiHA antibody specifically detected HA-tagged $\delta2^{wt}$ receptors on the surface of HEK293 cells. No staining was detected with the antiHA antibody when $\delta2^{wt}$ receptor with an HA tag at the C-terminus was expressed in HEK293 cells, a result confirming the specific binding of the antibody to surface proteins under this condition (data not shown). Although most $\delta2^{wt}$ receptors were located on the cell surface, we detected very few cells expressing the mutant $\delta2^{ho7J}$, $\delta2^{ho11J}$ or $\delta2^{ho9J}$ receptors on the surface (Fig. 5A). This result indicates that the deleted regions are important for transport of δ2 receptors to the cell surface.

To determine why the mutant δ2 receptor proteins were not transported to the surface of HEK293 cells, we treated δ2 receptor proteins with Endo H, which removes unprocessed high-mannose oligosaccharides from proteins that reside in the ER and *cis*-Golgi. The $\delta2^{wt}$ receptors expressed in HEK293 cells and immunoprecipitated with an antiδ2 receptor antibody were only partially digested by Endo H treatment (Fig. 5B), a finding that is consistent with an earlier report that δ2 receptors are efficiently transported to the plasma membrane (Matsuda & Mishina, 2000). However, the high-mannose oligosaccharides on the $\delta2^{ho7J}$, $\delta2^{ho11J}$ and $\delta2^{ho9J}$ receptors were completely digested by Endo H, as indicated by the increase in electrophoretic

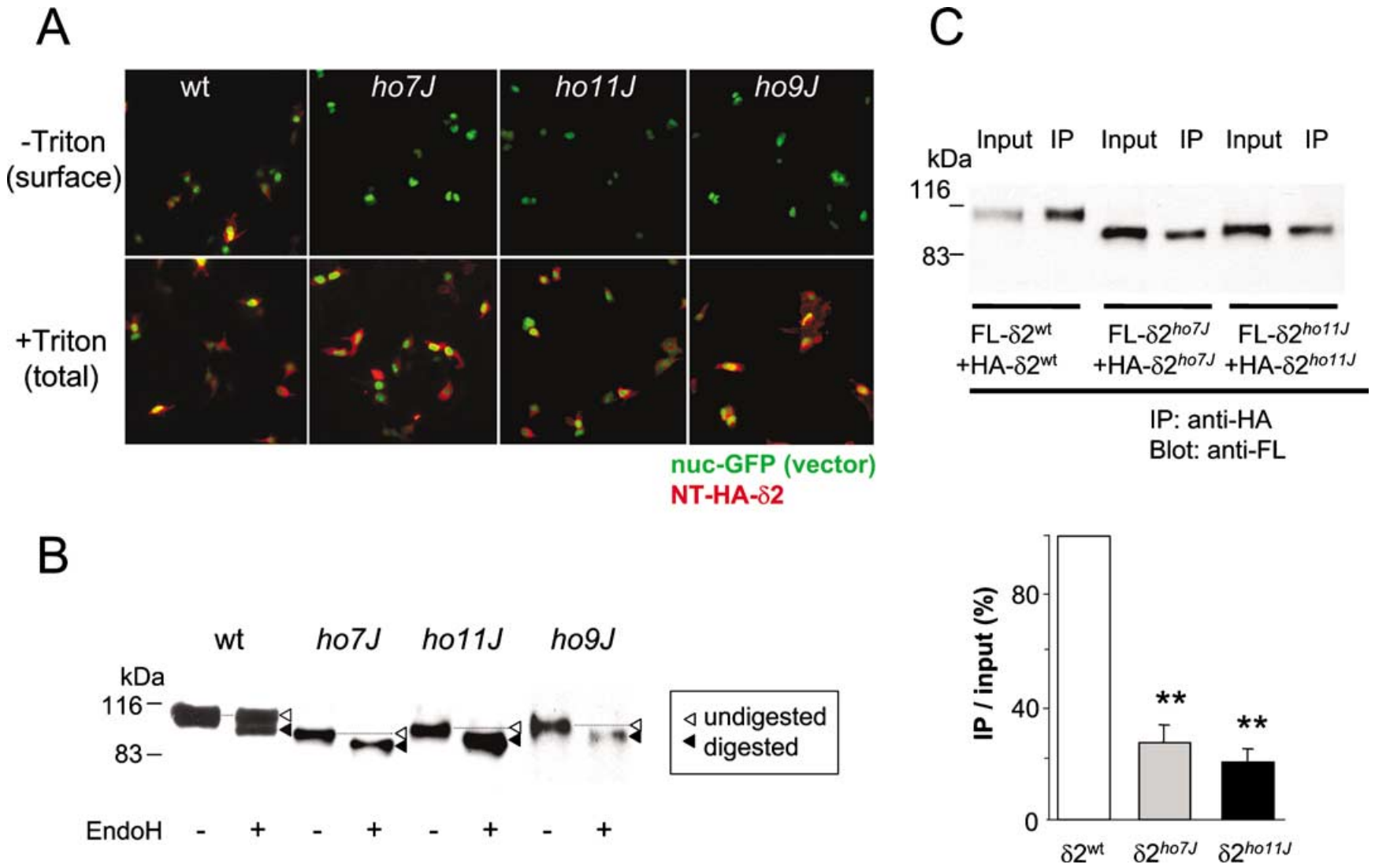

FIG. 5. Effects of deletions found in the *ho7J, ho11J* and *ho9J* alleles on the functions of δ2 receptors. (A) Immunocytochemical analysis of expression of δ2 receptors on the cell surface. Each construct contained δ2 receptor cDNA whose 5′ end was tagged with a region encoding HA (NT-HA-δ2); each construct was expressed in HEK293 cells. Expression of these receptors on the cell surface was examined by using an antiHA antibody (red) under nonpermeabilizing conditions (upper panels). The proportion of HA^+ cells among the transfected cells, which were identified by the green fluorescence of GFP in the nucleus (nuc-GFP), was $78 \pm 5\%$ for cells expressing $\delta2^{wt}$, $8 \pm 3\%$ for cells expressing $\delta2^{ho7J}$, $7 \pm 4\%$ for cells expressing $\delta2^{ho11J}$ and $6 \pm 4\%$ for cells expressing $\delta2^{ho9J}$ ($n = 90$ cells from three independent experiments). Lower panels show the staining pattern under permeabilizing conditions (control). (B) Sensitivity to Endo H digestion. Wt or *hotfoot* δ2 receptors were expressed in HEK293 cells, immunoprecipitated with antiδ2 antibody, and treated with Endo H. Lanes 1 and 2 show the results of treatment of $\delta2^{wt}$ receptors; lanes 3 and 4, $\delta2^{ho7J}$ receptors; lanes 5 and 6, $\delta2^{ho11J}$ receptors; lanes 7 and 8, $\delta2^{ho9J}$ receptors. (C) Coimmunoprecipitation of FLAG-tagged and HA-tagged receptors. FLAG-tagged and HA-tagged δ2 receptors were coexpressed in HEK293 cells and were immunoprecipitated (IP) with anti-HA antibody. Blots of the immunoprecipitates were analysed with anti-FLAG antibody. 'Input' indicates those lanes containing the lysate fraction; 'IP', those containing the immunoprecipitates. The combinations of plasmids transfected into the cells are indicated. Results of a quantitative analysis of the relative amounts of the coimmunoprecipitated δ2 receptors are shown in a graph. The bar shows the mean band intensities ($n = 4$). Error bars indicate SEM. The amount of coimmunoprecipitated FLAG-tagged $\delta2^{wt}$ receptors was significantly larger than the amount of coimmunoprecipitated FLAG-tagged *hotfoot* δ2 receptors. $^{**}P < 0.01$, comparing the percentages of immunoprecipitated $\delta2^{wt}$ and *hotfoot* δ2 receptors.

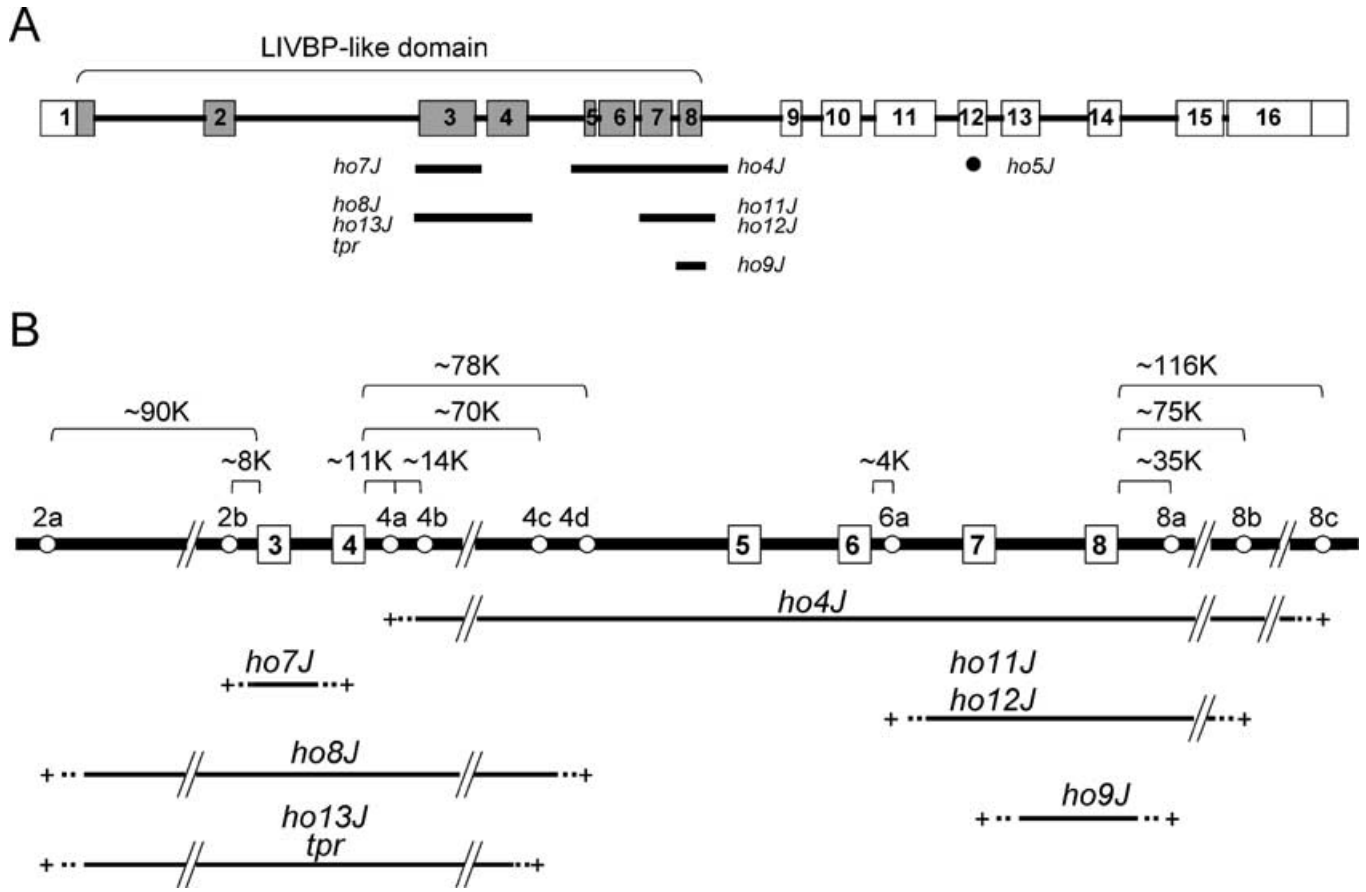

FIG. 6. Schematic representation of various *hotfoot* mutations in the *Grid2* gene. (A) *Ho4J* and *hotfoot* mutations identified in this study of the *Grid2* gene. Exons encoding the LIVBP-like domain of δ2 receptors are indicated by shaded boxes. Except for a point mutation in the *ho5J* allele (●), large deletions (–) in other *hotfoot* alleles are in the region encoding the LIBVP-like domain. (B) An enlarged view of the region of the *Grid2* gene where most *hotfoot* mutations occur. Exons are indicated by boxes. PCR markers (see Table 1 for sequences and locations of primers) in introns are indicated by ○, together with their distance from the nearby exons. The plus symbol (+) indicates that the PCR marker is present in the *hotfoot* allele. A broken line (- -) at the start or end of each deletion indicates that the deletion starts or ends near this region of the *Grid2* gene.

mobility of the receptors (Fig. 5B). Therefore, the regions within the LIVBP-like domain that are absent in $\delta2^{ho7J}$, $\delta2^{ho11J}$ and $\delta2^{ho9J}$ receptors are crucial for the exit of δ2 receptors from the ER and *cis*-Golgi. Abnormal transport of mutant δ2 receptors was further confirmed by immunocytochemical analysis of COS-7 cells. Although $\delta2^{wt}$ receptors were detected outside the ER, the fluorescence pattern of mutant δ2 receptors completely overlapped that of the ER-resident chaperone protein calnexin in COS-7 cells (data not shown).

The expression of receptors on the cell surface is regulated by the quality control mechanism in the ER. Many multimeric receptor channels are preassembled in the ER, but only those complexes that are assembled properly can exit the ER and be inserted into the cell surface (Griffon *et al*., 1999; Zerangue *et al*., 1999; Standley *et al*., 2000). To analyse the oligomerization of mutant δ2 receptors, we transfected HEK293 cells with expression vectors for HA- or FLAG-tagged $\delta2^{wt}$, $\delta2^{ho7J}$ or $\delta2^{ho11J}$ receptors, and immunoprecipitated them with an antiHA antibody. Western blots of the immunoprecipitates were incubated with the anti-FLAG antibody. The amount of FLAG-tagged $\delta2^{ho7J}$ receptors that coimmunoprecipitated with HA-tagged $\delta2^{ho7J}$ receptors was significantly lower than that of FLAG-tagged $\delta2^{wt}$ receptors that coimmunoprecipitated with HA-tagged $\delta2^{wt}$ receptors (Fig. 5C). We obtained similar results with $\delta2^{ho11J}$ and $\delta2^{ho9J}$. The interaction between these mutant δ2 receptors was as weak as that between AMPA receptor GluR1 and kainate receptor GluR6 (Matsuda & Yuzaki, 2002), which do not coassemble into functional receptors even in heterologous cells (Ayalon & Stern-Bach, 2001). These results indicate that the *ho7J*, *ho11J* and *ho9J* mutations in the LIVBP-like domain significantly decreased the interaction between individual δ2 receptors to a level at which no functional channels are formed. Reduced intermolecular interaction may contribute to the retention of the mutant receptors in the ER, leading to reduction in the number of receptors on the cell surface and the appearance of the ataxic phenotype.

Start and endpoints of deletions in Grid2 *of* hotfoot *mice*

Interestingly, most mutations in the *hotfoot* mutants analysed in the present study involve the deletion of one or more exons (Fig. 6A). One possible explanation for this phenomenon is that the *Grid2* gene contains several fragile sites. For example, as four deletions begin in intron 2 (Fig. 6A), this region of the *Grid2* gene may be fragile. To test this hypothesis, we performed low-resolution mapping of the deletions by testing for the intronic PCR markers shown in Fig. 6B. The *ho7J* deletion begins in intron 2 within 8 kb upstream of exon 3, whereas the deletions in *ho8J*, *ho13J* and *tpr* alleles begin further upstream (Fig. 6B). The *ho8J* deletion ends in intron 4, between 70 and 78 kb downstream of exon 4, while the deletions in *ho13J and tpr* mice end between 14 and 70 kb downstream of the exon. These deletion endpoints in intron 4 are distinct from the start of the *ho4J* deletion,

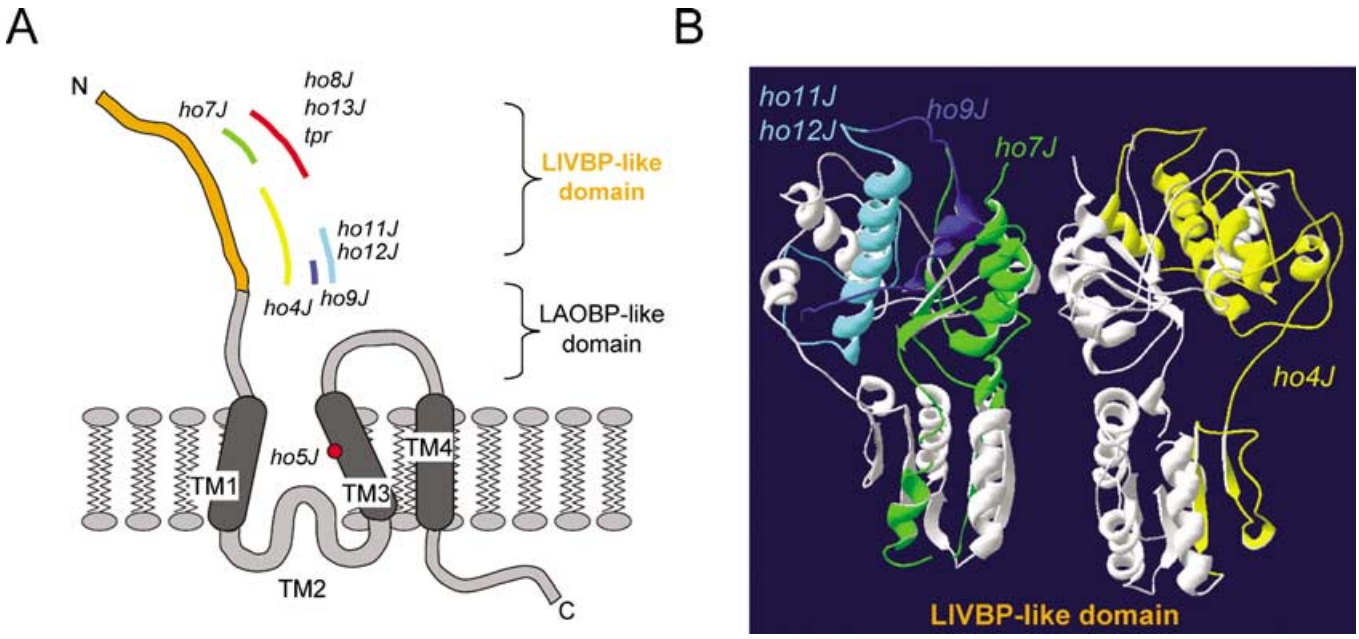

FIG. 7. Schematic representation of various *hotfoot* mutations in δ2 receptor proteins. (A) Presumed membrane topology of δ2 receptors. The LIVBP-like domain is at the N-terminus. The bipartite lysine/arginine/ornithine-binding protein (LAOBP)-like domain, whose subregions are separated by transmembrane domains 1–3 (TM1–TM3), form the agonist-binding pocket. Except for a point mutation in the *ho5J* allele in the TM3 (●), large deletions (–) in other *hotfoot* alleles occurred in the LIBVP-like domain. (B) Structural model of the LIVBP-like domain of the δ2 receptor. The green region, which corresponds to the dimer interface, indicates amino acids deleted in the *ho7J* allele. The blue and the light blue regions indicate the *ho11J* or *ho12J* region, and the blue region indicates the *ho9J* region. The region deleted in the *ho4J* allele (Matsuda & Yuzaki, 2002) was also shown in yellow for comparison. These regions underlie the interface responsible for dimerization.

which is located 11–14 kb downstream of exon 4. Likewise, the endpoints of the *ho4J*, *ho11J* and *ho9J* deletions in intron 8 are not identical. Our results suggest that there are no common fragile sites for deletions in *Grid2* (Fig. 6B).

Discussion

Exon deletion in Grid2 *alleles*

PCR analysis of genomic DNA identified the alterations in the *Grid2* gene of eight types of *hotfoot* mice: *ho5J*, *ho7J*, *ho8J*, *ho9J, ho11J*, *ho12J*, *ho13J* and *tpr*. Except for the *ho5J* allele (which had a point mutation in exon 12), all *hotfoot* mutants had deletions of one or more exons coding for portions of the LIVBP-like domain of the δ2 receptor (Fig. 7A). Because for several alleles we could only analyse genomic DNA, it is difficult to rule out the possibility that the loss of a part of an intron can affect the splicing of other exons or the general efficiency of transcription of the δ2 receptor gene. However, the agreement between the results of PCR of genomic DNA, RT-PCR and immunoblot analysis in the cases of the *ho4J, ho5J* and *tpr* alleles indicates that the analysis of genomic DNA can often predict the effects on mRNA and protein.

The region encoding the LIVBP-like domain: a hot spot for mutations in hotfoot *mice*

Why do many deletions occur in exons that encode the LIVBP-like domain of δ2 receptors? A possible explanation is that the presence of fragile sites in this region of the *Grid2* gene. However, multiple distinct start and endpoints were identified for deletions within this region (Fig. 6B). Another possible reason for the frequent occurrence of deletions is that introns in this region are generally larger than those outside this region, and it accounts for two-thirds of the gene. For example, four *hotfoot* deletions begin in intron 2, the largest intron of *Grid2* (Fig. 6A). However, this theory cannot fully explain the frequent occurrence of mutations in small introns within the LIVBP-like domain: intron 3 (*ho7J*), intron 6 (*ho11J* and *12 J*) and intron 7 (*ho9J*). In addition, all five in-frame *hotfoot* mutations are found within the LIVBP-like domain, a result suggesting that in-frame mutations outside this domain may not result in the null (*hotfoot*) phenotype. Therefore, we suggest that although mutations occur randomly all over the *Grid2* gene, those affecting the LIVBP-like domain are more frequently associated with the *hotfoot* phenotype.

Function of the LIVBP-like domain

We recently demonstrated that the *ho4J* mutation in the region encoding the LIVBP-like domain inhibits the function of δ2 receptors by impairing the receptors' exit from the ER, and thus their transport and placement on the surface of Purkinje cells (Matsuda & Yuzaki, 2002). In the present study, we found that *ho7J*, *ho11J, ho12J* and *ho9J* mutations in the region coding for the LIVBP-like domain also resulted in the failure of δ2 receptors to exit the ER and reside on the surface of HEK293 cells. These results are consistent with the view that δ2 receptor proteins need to be transported to the cell surface to function and that mutations that impair this process result in the ataxic phenotype of the *hotfoot* mice.

Although the deletion in $\delta2^{ho7J}$ receptors (95 amino acids), $\delta2^{ho11J}$ receptors (94 amino acids) and $\delta2^{ho9J}$ receptors (40 amino acids) is much smaller than that in $\delta2^{ho4J}$ receptors (170 amino acids), we found that, like the *ho4J* deletion, these smaller deletions in the region encoding the LIVBP-like domain significantly decreased the interaction between individual δ2 receptors to a level at which no functional channels were formed. Because LIVBP-like domains of various receptors, including those of GluR4 (Kuusinen *et al*., 1999) and metabotropic glutamate receptors (Kunishima *et al*., 2000), tend to dimerize with each other, it has been hypothesized that a major

function of this domain in ionotropic glutamate receptors is oligomerization of subunits. Interestingly, all deletions in the LIVBP-like domain of δ2 receptors in *hotfoot* mice correspond to the interface for dimerization, or the structure that underlies the interface, on a three-dimensional model (Fig. 7B). Therefore, we speculate that these deletions impair the oligomerization of δ2 receptors in *hotfoot* mice by disrupting the proper orientation of the dimer interface.

Many multimeric receptor channels are preassembled in the ER where assembly is tightly coupled to the trafficking of their individual components to prevent monomers and incompletely assembled complexes from reaching the cell surface (Griffon *et al*., 1999; Zerangue *et al*., 1999; Standley *et al*., 2000). Because the *hotfoot* deletions reduced the interactions between δ2 receptor subunits and the transport of complexes to the cell surface, we propose that weakly associated δ2 receptor complexes, which probably have several conformations or misfolding of the N-terminus, are detected by ER-resident chaperones and retained in the ER. Because the deletions are in the N-terminus of the δ2 receptor, the quality control mechanism may involve proteins located in the ER lumen. Alternatively, the LIVBP-like domain of δ2 receptors may possess a specific signal recognized by unidentified protein-trafficking mechanisms, as reported recently for GluR1 and GluR2 (Xia *et al*., 2002). In this case, the *hotfoot* deletions may impair the proper presentation of this motif to the trafficking machinery. It has become increasingly clear that glutamatergic signalling is mainly modulated *in vivo* by membrane-trafficking processes controlling the expression of receptors on the cell surface (Malinow & Malenka, 2002). Indeed, our results clearly indicate the importance of the LIVBP-like domain in the function of δ2 receptors *in vivo*. Therefore, further studies are warranted to better characterize the mechanisms of the LIVBP-like domains in controlling the trafficking of ionotropic glutamate receptors.

Acknowledgements

We thank J. Boulter for the gift of the cDNAs that encoded δ2 receptors; H. Hirai, Y. Kamiya and K. Matsuda for useful discussions and J.C. Jones for her editorial assistance. This work was supported in part by the Japan Society for the Promotion of Science (JSPS) (S. M.), the National Institutes of Health grants NS36925 (M. Y.) and NS34509 (M. H. M.), the Cancer Center Support Grant CA21765, and the American Lebanese Syrian Associated Charities (M. Y.). V. D. acknowledges support from the Neuroscience Training Program of the University of Michigan (T32 MH14279).

Abbreviations

AMPA, α-amino-3-hydroxy-5-methyl-4 isoazolepropionic acid; Endo H, endoglycosidase H; ER, endoplasmic reticulum; GFP, green fluorescent protein; HA, haemagglutinin; HEK293 cells, human embryonic kidney 293 cells; LIVBP, leucine/isoleucine/valine-binding protein; NMDA, *N*-methyl-D-aspartate; PBS, phosphate-buffered saline; PCR, polymerase chain reaction; RT, reverse transcriptase; TM, transmembrane domain; *tpr*, *tapdancer*.

References

Araki, K., Meguro, H., Kushiya, E., Takayama, C., Inoue, Y. & Mishina, M. (1993) Selective expression of the glutamate receptor channel delta 2 subunit in cerebellar Purkinje cells. *Biochem. Biophys. Res. Commun.*, **197**, 1267–1276.

Ayalon, G. & Stern-Bach, Y. (2001) Functional assembly of AMPA and kainate receptors is mediated by several discrete protein–protein interactions. *Neuron*, **31**, 103–113.

Berquin, P.C., Giedd, J.N., Jacobsen, L.K., Hamburger, S.D., Krain, A.L., Rapoport, J.L. & Castellanos, F.X. (1998) Cerebellum in attention-deficit hyperactivity disorder: a morphometric MRI study. *Neurology*, **50**, 1087–1093.

Courchesne, E. (1999) An MRI study of autism: the cerebellum revisited. *Neurology*, **52**, 1106–1107.

Dickie, M.M. (1966) Hotfoot. *Mouse News Lett.*, **34**, 30.

Griffon, N., Buttner, C., Nicke, A., Kuhse, J., Schmalzing, G. & Betz, H. (1999) Molecular determinants of glycine receptor subunit assembly. *EMBO J.*, **18**, 4711–4721.

Kashiwabuchi, N., Ikeda, K., Araki, K., Hirano, T., Shibuki, K., Takayama, C., Inoue, Y., Kutsuwada, T., Yagi, T., Kang, Y., Aizawa, S. & Mishina, M.. (1995) Impairment of motor coordination, Purkinje cell synapse formation, and cerebellar long-term depression in GluR delta 2 mutant mice. *Cell*, **81**, 245–252.

Kohda, K., Wang, Y. & Yuzaki, M. (2000) Mutation of a glutamate receptor motif reveals its role in gating and delta2 receptor channel properties. *Nature Neurosci.*, **3**, 315–322.

Kunishima, N., Shimada, Y., Tsuji, Y., Sato, T., Yamamoto, M., Kumasaka, T., Nakanishi, S., Jingami, H. & Morikawa, K. (2000) Structural basis of glutamate recognition by a dimeric metabotropic glutamate receptor. *Nature*, **407**, 971–977.

Kuusinen, A., Abele, R., Madden, D.R. & Keinanen, K. (1999) Oligomerization and ligand-binding properties of the ectodomain of the alpha-amino-3-hydroxy-5-methyl-4-isoxazole propionic acid receptor subunit GluRD. *J. Biol. Chem.*, **274**, 28937–28943.

Lalouette, A., Guenet, J.L. & Vriz, S. (1998) Hotfoot mouse mutations affect the delta 2 glutamate receptor gene and are allelic to lurcher. *Genomics*, **50**, 9–13.

Lalouette, A., Lohof, A., Sotelo, C., Guenet, J. & Mariani, J. (2001) Neurobiological effects of a null mutation depend on genetic context: comparison between two hotfoot alleles of the delta-2 ionotropic glutamate receptor. *Neurosci.*, **105**, 443–455.

Landsend, A.S., Amiry-Moghaddam, M., Matsubara, A., Bergersen, L., Usami, S., Wenthold, R.J. & Ottersen, O.P. (1997) Differential localization of delta glutamate receptors in the rat cerebellum: coexpression with AMPA receptors in parallel fiber-spine synapses and absence from climbing fiber-spine synapses. *J. Neurosci.*, **17**, 834–842.

Lomeli, H., Sprengel, R., Laurie, D.J., Kohr, G., Herb, A., Seeburg, P.H. & Wisden, W. (1993) The rat delta-1 and delta-2 subunits extend the excitatory amino acid receptor family. *FEBS Lett.*, **315**, 318–322.

Malinow, R. & Malenka, R.C. (2002) AMPA receptor trafficking and synaptic plasticity. *Annu. Rev. Neurosci.*, **25**, 103–126.

Matsuda, I. & Mishina, M. (2000) Identification of a juxtamembrane segment of the glutamate receptor delta2 subunit required for the plasma membrane localization. *Biochem. Biophys. Res. Commun.*, **275**, 565–571.

Matsuda, S. & Yuzaki, M. (2002) Mutation in hotfoot-4J mice results in retention of d2 glutamate receptors in ER. *Eur. J. Neurosci.*, **16**, 1507–1516.

Nicolson, R., Fawcett, A.J. & Dean, P. (2001) Dyslexia, development and the cerebellum. *Trends Neurosci.*, **24**, 515–516.

Standley, S., Roche, K.W., McCallum, J., Sans, N. & Wenthold, R.J. (2000) PDZ domain suppression of an ER retention signal in NMDA receptor NR1 splice variants. *Neuron*, **28**, 887–898.

Truett, G.E., Heeger, P., Mynatt, R.L., Truett, A.A., Walker, J.A. & Warman, M.L. (2000) Preparation of PCR-quality mouse genomic DNA with hot sodium hydroxide and tris (HotSHOT). *Biotechniques*, **29**, 52, 54.

Xia, H., Von Zastrow, M. & Malenka, R.C. (2002) A novel anterograde trafficking signal present in the N terminal extracellular domain of ionotropic glutamate receptors. *J. Biol. Chem.*, **3**, 3.

Zerangue, N., Schwappach, B., Jan, Y.N. & Jan, L.Y. (1999) A new ER trafficking signal regulates the subunit stoichiometry of plasma membrane K (ATP) channels. *Neuron*, **22**, 537–548.

Zuo, J., De Jager, P.L., Takahashi, K.A., Jiang, W., Linden, D.J. & Heintz, N. (1997) Neurodegeneration in Lurcher mice caused by mutation in delta2 glutamate receptor gene. *Nature*, **388**, 769–773.